# Appendix

## Autophagy regulates neuronal excitability by controlling cAMP/Protein Kinase A signaling at the synapse

Overhoff M., Tellkamp F., Hess S., Tolve M., Tutas J., Faerfers M., Ickert L., Mohammadi M., De Bruyckere E., Kallergi E., Delle Vedove A., Nikoletopoulou V., Wirth B., Isensee J., Hucho T., Puchkov D., Isbrandt D., Krüger M., Kloppenburg P., Kononenko N.L.*

*Corresponding author. Email: n.kononenko@uni-koeln.de

**This PDF file includes:**

# Extended figures

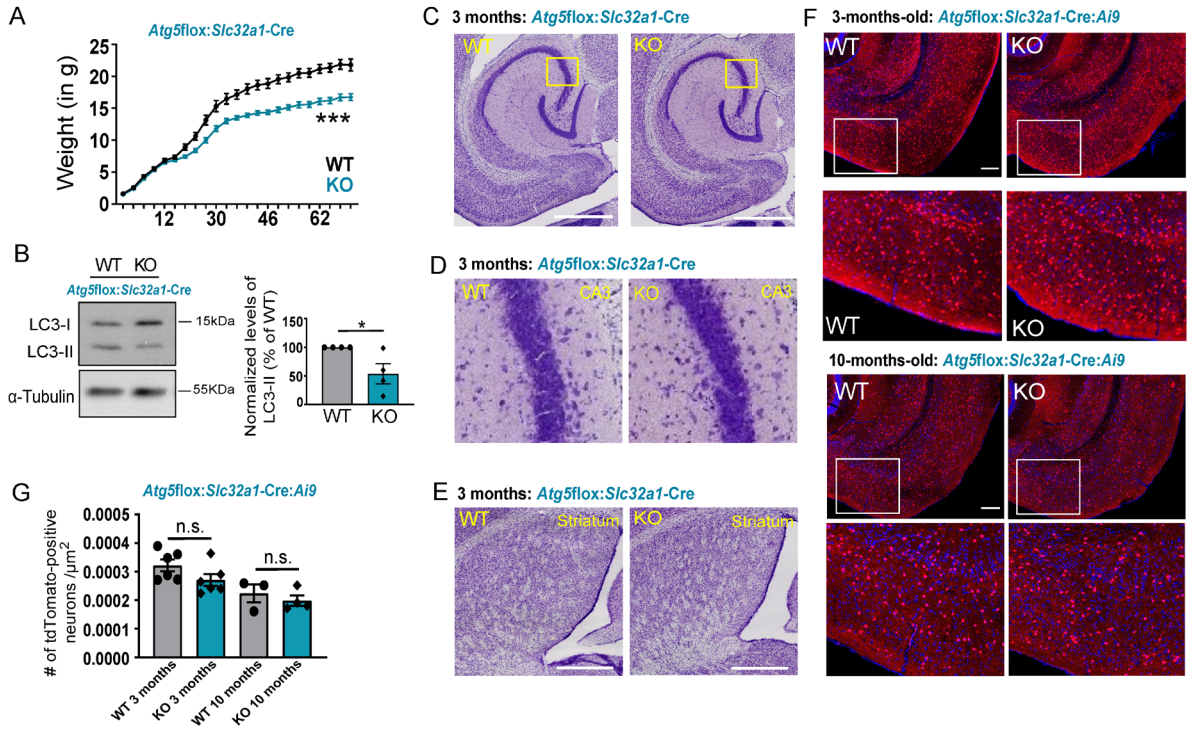


H

| | | Atg5flox: CamKIIa-Cre, WT (N=8) | | Atg5flox: CamKIIa-Cre, KO (N=9) | | Mann-Whitney test |
|---|---|---|---|---|---|---|
| | | mean | SD | mean | SD | p Value |
| Viewing jar | Activity | 1 | 0 | 1 | 0 | n.s. |
| | Tremor | 0 | 0 | 0.333333 | 0.5 | n.s. |
| | Defecation | 1 | 0 | 1 | 0 | n.s. |
| | Urination | 0.75 | 0.46291 | 0.555556 | 0.527046 | n.s. |
| | Lacrimation | 0 | 0 | 0 | 0 | n.s. |
| | Palpebral closure | 0 | 0 | 0 | 0 | n.s. |
| | Number of rear | 10.5 | 6.969321 | 7.888889 | 4.013865 | n.s. |
| Arena | Transfer arousal | 2 | 0 | 1.888889 | 0.333333 | n.s. |
| | Locomotor activity | 34.375 | 13.94825 | 37.22222 | 19.81652 | n.s. |
| | Gait | 0 | 0 | 0.111111 | 0.333333 | n.s. |
| | Pelvic elevation | 0.625 | 0.517549 | 0.666667 | 0.5 | n.s. |
| | Tail elevation | 1.25 | 0.46291 | 1.111111 | 0.600925 | n.s. |
| | Startle response | 0.875 | 0.353553 | 1.555556 | 0.527046 | **0.0204** |
| | Touch escape | 0.875 | 0.64087 | 1.444444 | 0.726483 | n.s. |
| Hold by tail | Struggle | 0 | 0 | 0 | 0 | n.s. |
| | Trunk Curl | 0 | 0 | 0 | 0 | n.s. |
| | Limb grasping | 0 | 0 | 0 | 0 | n.s. |
| hold by neck | Struggle | 0 | 0 | 0 | 0 | n.s. |
| other | Corneal reflex | 1 | 0 | 1 | 0 | n.s. |
| | Tail pinch | 1 | 0 | 0.833333 | 0.408248 | n.s. |
| | Biting | 1 | 0 | 1 | 0 | n.s. |
| | Vocalisation | 1 | 0 | 1 | 0 | n.s. |

I

| | | Atg5flox: Slc32a1-Cre, WT (N=9) | | Atg5flox: Slc32a1-Cre, KO (N=11) | | Mann-Whitney test |
|---|---|---|---|---|---|---|
| | | mean | SD | mean | SD | p Value |
| Viewing jar | Activity | 1 | 0 | 1 | 0 | n.s. |
| | Tremor | 0 | 0 | 0.363636 | 0.504452 | n.s. |
| | Defecation | 1 | 0 | 0.909091 | 0.301511 | n.s. |
| | Urination | 1 | 0 | 0.545455 | 0.522233 | **0.0379** |
| | Lacrimation | 0 | 0 | 0 | 0 | n.s. |
| | Palpebral closure | 0 | 0 | 0 | 0 | n.s. |
| | Number of rear | 12.77778 | 5.190804 | 6.818182 | 5.688905 | **0.0227** |
| Arena | Transfer arousal | 1.888889 | 0.333333 | 2 | 0 | n.s. |
| | Locomotor activity | 30.88889 | 8.038104 | 31.63636 | 14.30575 | n.s. |
| | Gait | 0 | 0 | 0.545455 | 0.522233 | **0.0141** |
| | Pelvic elevation | 1 | 0 | 0.909091 | 0.301511 | n.s. |
| | Tail elevation | 1 | 0 | 0.909091 | 0.700649 | n.s. |
| | Startle response | 1.111111 | 0.333333 | 2 | 0 | **<0.0001** |
| | Touch escape | 1.444444 | 0.527046 | 1.545455 | 0.687552 | n.s. |
| Hold by tail | Struggle | 0 | 0 | 0 | 0 | n.s. |
| | Trunk Curl | 0 | 0 | 0 | 0 | n.s. |
| | Limb grasping | 0 | 0 | 0 | 0 | n.s. |
| hold by neck | Struggle | 0 | 0 | 0 | 0 | n.s. |
| other | Corneal reflex | 1 | 0 | 1 | 0.301511 | n.s. |
| | Tail pinch | 1 | 0 | 0.909091 | 0.301511 | n.s. |
| | Biting | 1 | 0 | 0.9 | 0.40452 | n.s. |
| | Vocalisation | 1 | 0 | 0.909091 | 0.301511 | n.s. |

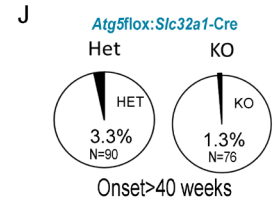

**Appendix Figure S1 | Phenotyping of mice lacking ATG5 in excitatory and inhibitory neurons. (A)** Bodyweight of *Atg5*flox:*Slc32a1*-Cre KO mice is decreased compared to WT littermates starting at 3 weeks of age (WT: 20.6± 0.68 g; KO: 15.6± 0.43 g at 2 month of age). p=<0.0001, $n_{WT}$=18, $n_{KO}$=20, two-tailed unpaired t-test. **(B)** Protein levels of lipidated LC3 (LC3-II) are reduced in striatal lysates of *Atg5*flox:*Slc32a1*-Cre KO mice compared to the WT set to 100% (WT set to 100%, KO: 53.69 ± 17.69%). p=0.0199; n=4, unpaired one-tailed t-test. **(C-E)** Nissl staining of 40 µM thick horizontal brain sections reveals no signs of neuronal cell loss in 12-week-old *Atg5*flox:*Slc32a1*-Cre KO mice neither in the CA1 region of the hippocampus (C, D) nor in striatum (E). Scale bar: 200µm. **(F, G)** The number of tdTomato-expressing neurons was not altered in the entorhinal cortex (white rectangle) of *Atg5*flox:*Slc32a1*-Cre:*Ai9* KO mice compared to the WT at 3 and 10 months of age ($WT_{3\ months}$: 0.00032± 0.00002079, n=6; $KO_{3\ months}$: 0.00027± 0.00002083, n=6; $WT_{10\ months}$: 0.00022± 0.00003156, n=3; $KO_{10\ months}$: 0.00020± 0.00001817, n=4, two-way ANOVA with Tukey's multiple comparisons test. Scale bar: 200µm. Sections were co-stained with DAPI shown in blue. **(H, I)** Results from the SHIRPA primary screening score performed with *Atg5*flox:*CamKIIα*-Cre WT/KO (H) and *Atg5*flox:*Slc32a1*-Cre WT/KO (I) mice. Analysis was performed with littermates at 13 weeks of age. **(J)** Percentages of *Atg5*flox:*Slc32a1*-Cre KO and HET mice that developed seizures at the age of 40 weeks and later. Animal number and the percentage of affected animals are displayed in the graphs (WT is set to 100%).

Data information: *P < 0.05; **P < 0.01; ***P < 0.001. All data represent mean ± SEM (Data in H, J are mean± SD). All n represent biological replicates.

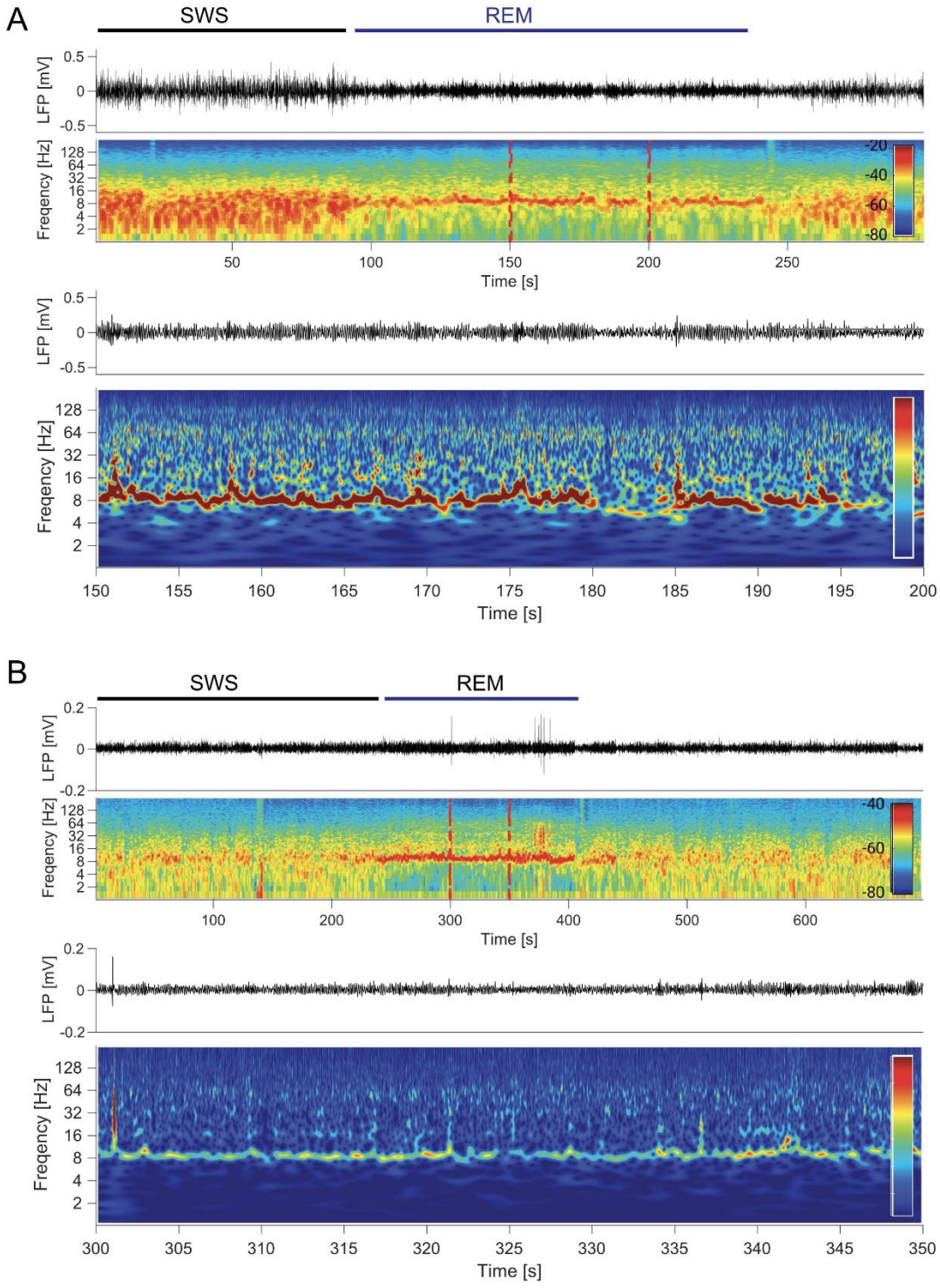


**Appendix Figure S2** | Examples of physiological ECoG sleep patterns during transitions from slow-wave sleep (SWS) to REM sleep in wildtype and Atg5flox:CamKIIα-Cre KO mice.

(**A**) Representative ECoG trace and corresponding multitaper spectrogram (top two panels) during the transition from SWS to REM sleep in a wild-type mouse obtained during chronic radiotelemetry recordings. A zoomed-in trace and corresponding wavelet spectrogram of the REM period indicated by red dotted lines in the multitaper spectrogram are shown in the bottom two panels. (**B**) Representative ECoG trace during an SWS-REM transition recorded from an Atg5flox:CamKIIα-Cre mutant mouse and corresponding spectrograms as in (A) indicating the presence of physiological sleep ECoG patterns in Atg5flox:CamKIIα-Cre mutants that are comparable to wildtype controls.

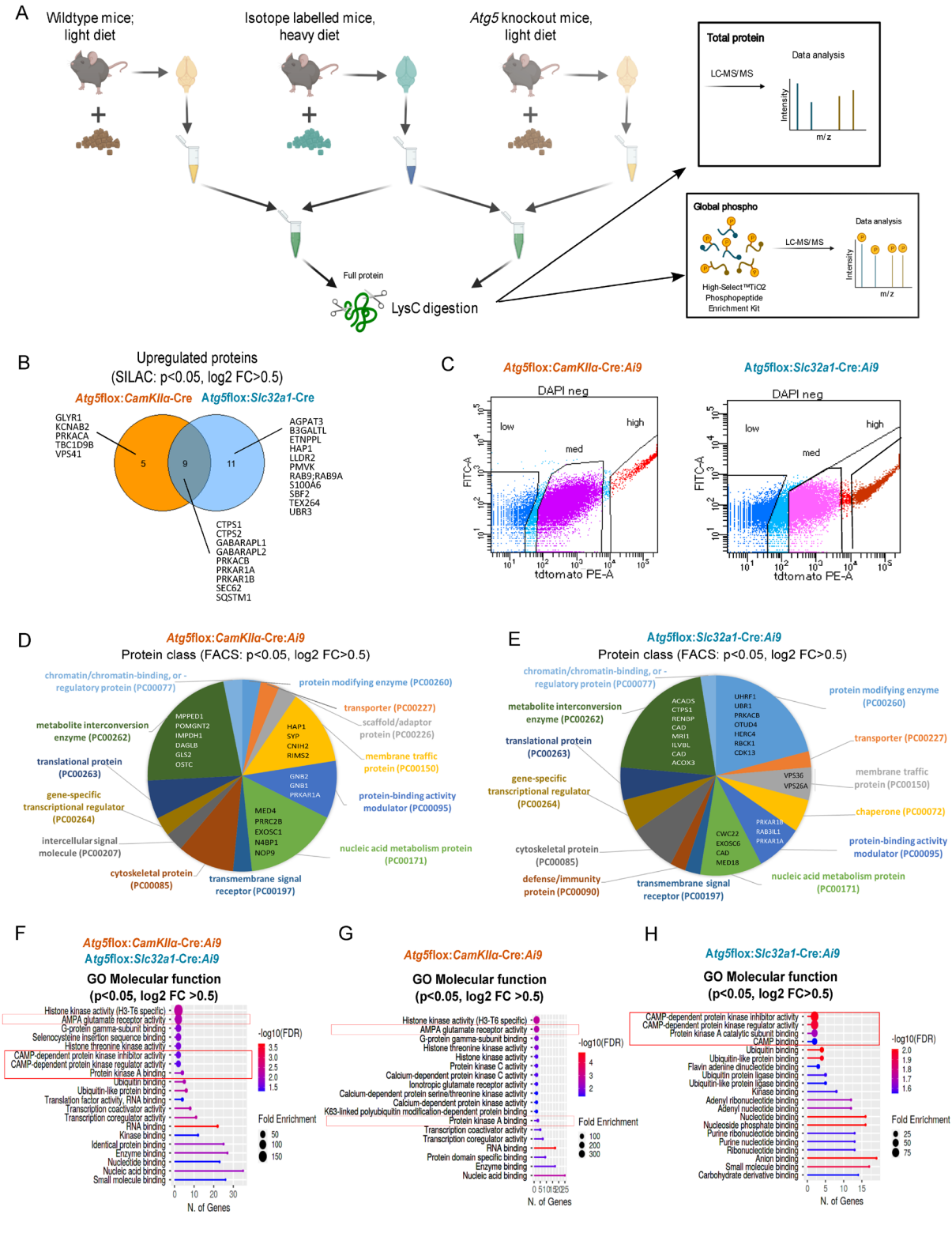


**Appendix Figure S3 | Proteome analysis of brains lacking ATG5 in excitatory and inhibitory neurons. (A)** Schematic illustration of SILAC spike-in approach for global proteome and

phosphoproteome analysis. Brain regions of interest from *Atg5*flox:*CamKIIα*-Cre (cortex) WT and KO mice, *Atg5*flox:*Slc32a1*-Cre (striatum) WT and KO mice and isotope-labeled mice (brain tissue) were dissected and homogenized. Unlabeled and isotope-labeled brain lysates were mixed in a 1:1 ratio and proteins were digested into peptides using LysC. Samples were divided to detect global proteome phosphoproteome alterations. **(B)** Venn diagram showing the number of highly upregulated proteins (log2FC>0.5, p<0.05) detected in SILAC spike-in global proteome analysis of *Atg5*flox:*CamKIIα*-Cre KO and *Atg5*flox:*Slc32a1*-Cre KO mice. **(C)** Exemplary illustration of fluorescence-based cell sorting (FACS) of *Atg5*flox:*CamKIIα*-Cre:*Ai9* and *Atg5*flox:*Slc32a1*-Cre:*Ai9* neurons. The cells were categorized in three populations depending on their tdTomato fluorescence intensity expression. Only the populations of highly tdTomato-positive cells were used for subsequent proteomic analysis. **(D, E)** Pie chart of protein classes upregulated (p<0.05, log2FC>0.5) in *Atg5*flox:*CamKIIα*-Cre:*Ai9* and *Atg5*flox:*Slc32a1*-Cre:*Ai9* FACS-sorted KO neurons, analyzed using Panther classification system (http://www.pantherdb.org/panther/ontologies.jsp). **(F-H)** ShinyGO v0.741-based gene ontology (GO) analysis of "molecular function"-enriched terms in the proteome of either pooled *Atg5*flox:*CamKIIα*-Cre:*Ai9* and *Atg5*flox:*Slc32a1*-Cre:*Ai9* datasets (F) or in the dataset obtained from *Atg5*flox:*CamKIIα*-Cre:*Ai9* (G) and *Atg5*flox:*Slc32a1*-Cre:*Ai9* (H) mice separately (cut-off p<0.05, log2 FC>0.5).

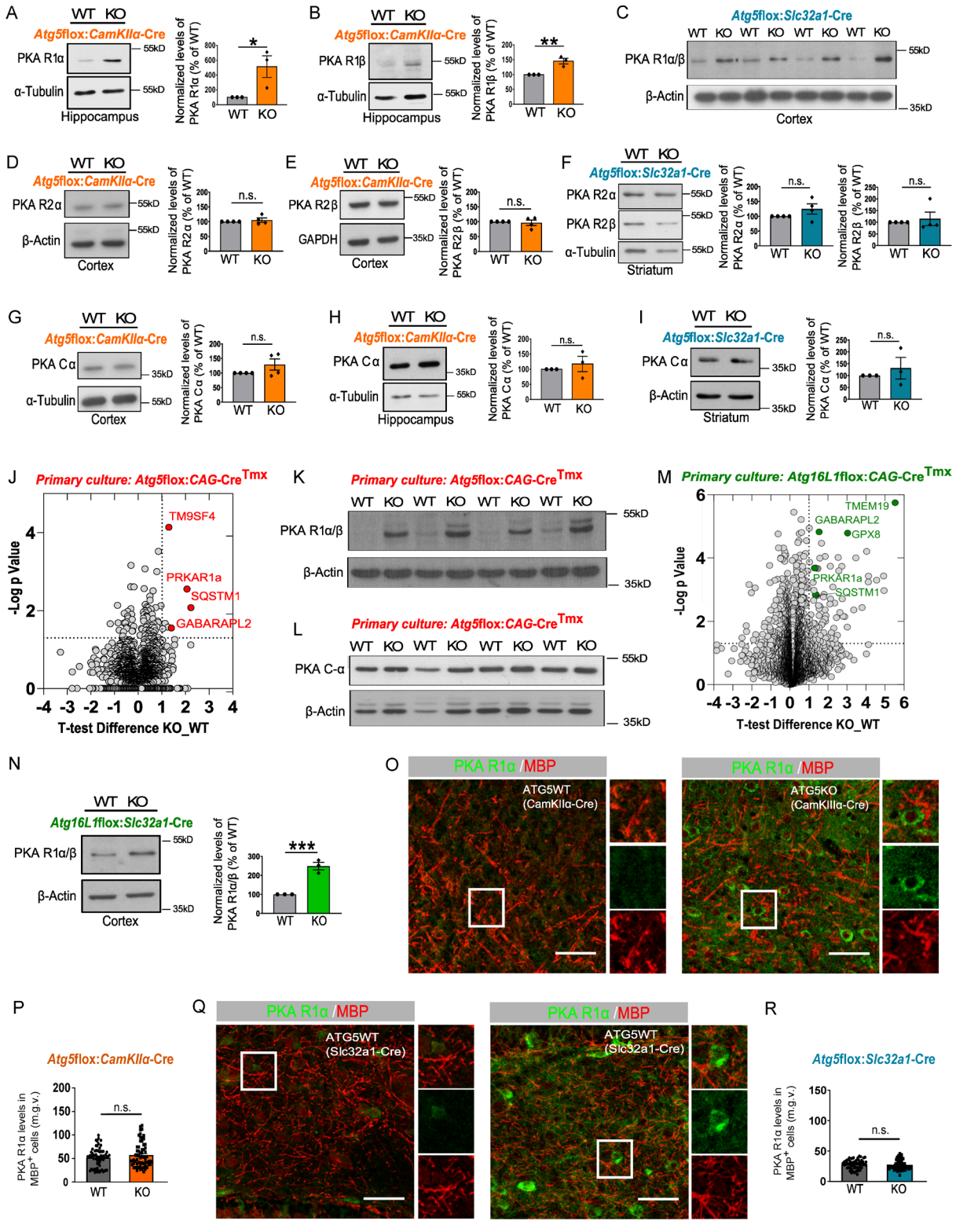


**Appendix Figure S4 | Levels of PKA R1α/β are upregulated in ATG5 and ATG16L1 KO neurons *in-vivo* and *in-vitro*. (A)** Protein levels of PKA R1α are significantly upregulated in

hippocampal brain lysates of Atg5flox:CamKIIα-Cre KO mice compared to the WT set to 100% (KO: 513.1± 146.8%). p= 0.0241, n=3. Performed one-tailed unpaired t-test. **(B)** Protein levels of PKA R1β are significantly upregulated in hippocampal brain lysates of Atg5flox:CamKIIα-Cre KO mice compared to the WT set to 100% (WT set to 100%, KO: 145.3± 9.578%). p= 0.0046, n=3. Performed one-tailed unpaired t-test. **(C)** Cortical lysates of *Atg5*flox:*Slc32a1*-Cre KO mice show increased PKA R1α/β protein levels in compared to the WT. **(D)** Protein levels of PKA R2α are unaltered in cortical brain lysates of *Atg5*flox:*CamKIIα*-Cre KO mice compared to the WT set to 100% (KO: 105.3± 7.399%). n=4. Performed one-tailed unpaired t-test. **(E)** Protein levels of PKA R2β are unaltered in cortical brain lysates of *Atg5*flox:*CamKIIα*-Cre KO mice compared to the WT set to 100% (KO: 96.40± 9.226%). n=4. Performed one-tailed unpaired t-test. **(F)** Protein levels of PKA R2α/β are unaltered in striatal brain lysates of *Atg5*flox:*Slc32a1*-Cre KO mice (PKA R2α KO: 124.6± 17.45%; PKA R2β KO: 114.6± 28.94%). n=4. Performed one-tailed unpaired t-test. **(G, H)** No upregulation of PKA Cα is observed in *Atg5*flox:*CamKIIα*-Cre KO neurons compared to the WT, neither in cortical (G) (KO: 129.1±19.39%, p=0.0921, n=4) nor hippocampal (H) brain lysates (KO: 117.6± 25.45%, p=0.2637, n=3). Performed one-tailed unpaired t-test. **(I)** In striatal brain lysates of *Atg5*flox:*Slc32a1*-Cre mice the PKA C-α was not changed compared to the WT (KO: 131.2± 45.27%). p=0.2644, n=3. Performed one-tailed unpaired t-test. **(J)** Volcano plot of differentially expressed proteins in *Atg5*flox:*CAG*-Cre$^{Tmx}$ primary cortical and hippocampal WT and KO neurons at DIV15-16 (n=3). **(K)** Western Blot analysis of PKA R1α/β protein levels in *Atg5*flox:*CAG*-Cre$^{Tmx}$ KO cortico-hippocampal primary neurons at DIV 15-16. **(L)** Western Blot analysis of PKA Cα protein levels in *Atg5*flox:*CAG*-Cre$^{Tmx}$ primary cortico-hippocampal WT and KO neurons at DIV15-16 (n=4). **(M)** Volcano plot of differentially expressed proteins in *Atg16L1*flox:*CAG*-Cre$^{Tmx}$ primary cortical and hippocampal WT and KO neurons at DIV15-16 (n=3). **(N)** Protein levels of PKA R1α/β are upregulated in cortical brain lysates of *Atg16L1*flox:*Slc32a1*-Cre KO mice compared to the WT (WT set to 100%, KO: 248.4± 19.64%). p=0.0008, n=3. Performed one-tailed unpaired t-test. **(O)** Immunohistochemistry for PKA R1α and MBP in the cortex of *Atg5*flox:*CamKIIα*-Cre WT and KO mice. White rectangular boxes indicate areas magnified to the right. Scale bar: 50µm. **(P)** Mean intensity of PKA R1α in MBP-positive cells is unaltered between *Atg5*flox:*CamKIIα*-Cre WT and KO mice (WT: 51.94±2.441, KO: 57.36±3.238; p=0.1804, two-tailed unpaired t-test). $n_{WT}$= 68; $n_{KO}$= 64 from n=3 mice. **(Q)** Immunohistochemistry for PKA R1α and MBP in the cortex of *Atg5*flox:*Slc32a1*-Cre

WT and KO mice. White rectangular boxes indicate areas magnified to the right. Scale bar: 50µm. **(R)** Mean intensity of PKA R1α in MBP positive cells is unaltered between *Atg5*flox:*Slc32a1*-Cre WT and KO mice (WT: 28.35±0.9838, KO: 27.09±0.8640; p=0.3388, two-tailed unpaired t-test). $n_{WT}$= 59; $n_{KO}$= 82 from n=3 mice.

Data information: *P < 0.05; **P < 0.01; ***P < 0.001. All data represent mean ± SEM. All n represent biological replicates.

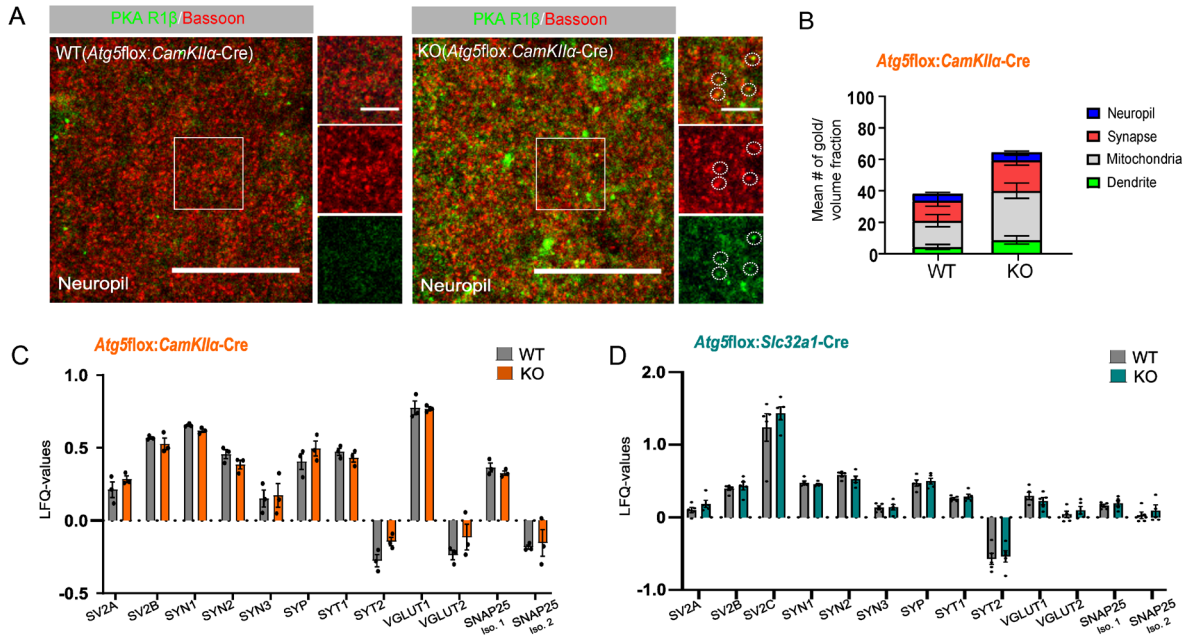


**Appendix Figure S5 | Bulk levels of SV proteins are unaltered in ATG5 KO brains. (A)** Immunohistochemistry for R1β and bassoon in cortical neuropil of *Atg5*flox:*CamKIIα*-Cre WT/ KO mice. White rectangular boxes indicate areas magnified to the right. Scale bar: 20µm, 5µm (inserts). White circles indicate R1β and bassoon colocalization in the KO. See also the quantification in Fig. 3F. **(B)** EM-based immunogold analysis reveals that PKA R1α/β is enriched at synapses (WT: 12.762± 3.625, KO: 19.323± 3.172), dendritic compartment (WT: 4.462± 1.539, KO: 8.869± 2.559) and mitochondria (WT: 16.618± 3.865, KO: 31.291± 4.829) of KO mice. Values display the mean number of gold particles per volume fraction from with $n_{WT}$=21 and $n_{KO}$=22 images analyzed with a grid size of 500k obtained from two mice for each genotype. **(C, D)** LFQ values of SV proteins from global proteome analysis of *Atg5*flox:*CamKIIα*-Cre (C) and *Atg5*flox:*Slc32a1*-Cre (D) WT and KO mice.

Data information: *P < 0.05; **P < 0.01; ***P < 0.001. All data represent mean ± SEM. All n represent biological replicates.

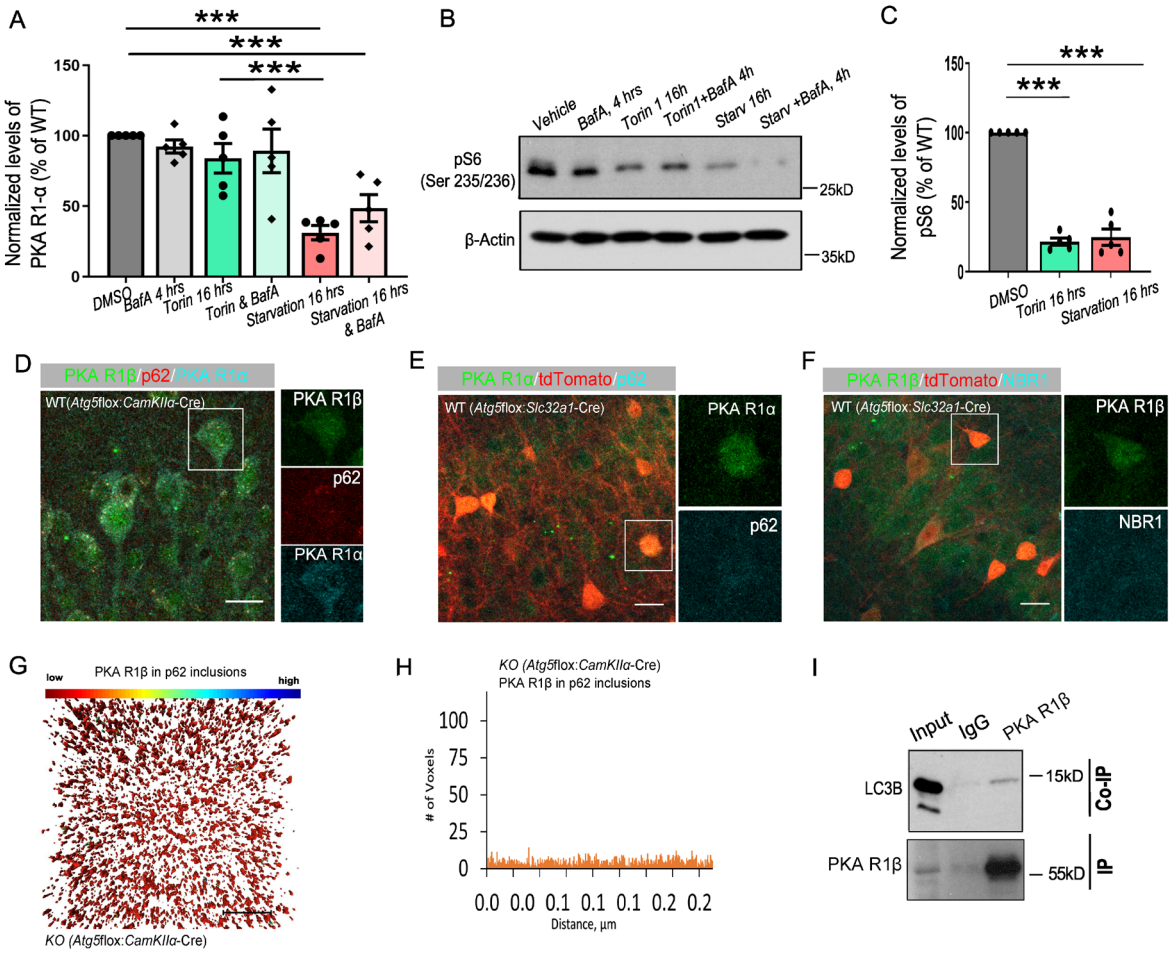


**Appendix Figure S6 | Starvation effect on PKA R1α is mTORC1-independent. (A)** Amino acids and serum starvation (16 hours), but not the mTORC1 inhibition by the Torin 1 (250nM, 16 hours) induces a decrease in PKA R1α total protein levels in NSC34 cells (DMSO: set to 100%, BafA 4 hours: 92.28± 4.612%, Torin 16 hours: 83.90± 10.48%, Torin & BafA: 89.15± 15.47%, Starvation 16 hours: 31.19± 5.085%, Starvation 16 hours & BafA: 48.52± 9.627%). $p_{DMSO/starvation\ 16\ hours}$<0,0001, $p_{Torin\ 16\ hours/starvation\ 16\ hours}$=0.0007, $p_{DMSO/starvation\ 16\ hours\ \&\ BafA}$=0.0009, n=5. Performed Two-Way ANOVA with Tukeys' multiple comparison test. **(B-C)** The levels of pS6 are equally reduced n NSC34 cells upon starvation and Torin 1 treatment (both 16h) (DMSO set to 100%, Torin 16 hours: 21.65± 2.541%, Starvation 16 hours: 24.82± 5.819%). $p_{DMSO/Torin\ 16\ hours}$<0.0001, $p_{DMSO/starvation\ 16\ hours}$<0.0001, n=5. Performed Two-Way ANOVA with Tukeys'

multiple comparison test. **(D-F)** Representative confocal images of the hippocampus CA1 area from *Atg5*flox:*CamKIIα*-Cre (D) and *Atg5*flox:*Slc32a1*-Cre (E,F) WT mice, immunostained for PKA R1α/β and co-immunostained for p62 and/or NBR1. White rectangular boxes indicate areas magnified to the right. Scale bar: 20µm. Representative pictures for KO are shown in Fig. 4K,L. **(G, H)** Uncropped image and analysis of the 3D-reconstruction shown in Fig. 4P (most right). Scale bar: 10 µm. The histogram in (H) shows the number of p62-labeled voxels (3D pixels) found within 250 nm of the PKA R1β neuropil staining. **(I)** Co-immunoprecipitation of endogenous PKA R1β with LC3 form *Atg5*flox:*CamKIIα*-Cre WT brain lysates. Input, 1.5% of the total lysate was added to the assay.

Data information: *P < 0.05; **P < 0.01; ***P < 0.001. All data represent mean ± SEM. All n represent biological replicates.

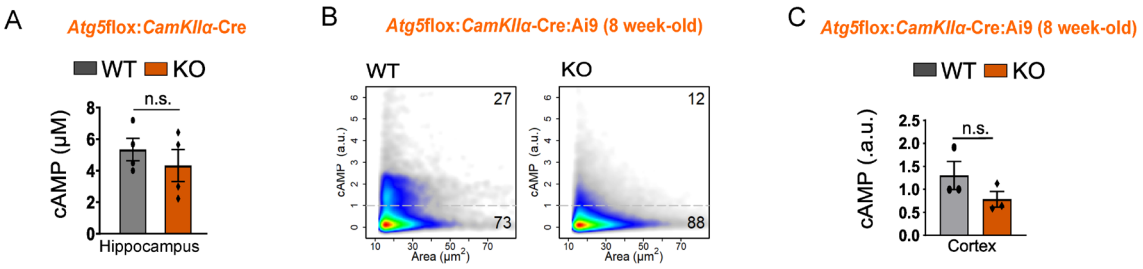


D

| log2 FoldChange | p-value | FDR | GENE ID | Description |
|---|---|---|---|---|
| 7.485700997 | 6.36852E-17 | 4.29614E-12 | *Gtf3c4* | general transcription factor IIIC, polypeptide 4 |
| 6.867994145 | 6.6644E-09 | 0.000149858 | *Srcap* | Snf2-related CREBBP activator protein |
| 6.625298107 | 3.12171E-07 | 0.00421175 | *Rev3l* | REV3 like, DNA directed polymerase zeta catalytic subunit |
| 6.60154495 | 4.4295E-08 | 0.000747025 | *Pdpk1* | 3-phosphoinositide dependent protein kinase 1 |
| 6.107961585 | 9.35384E-06 | 0.057363684 | *Brpf3* | bromodomain and PHD finger containing, 3 |
| 5.887685285 | 2.81595E-06 | 0.031660164 | *Adamtsl4* | ADAMTS-like 4 |
| 5.80575281 | 1.82371E-05 | 0.09463526 | *Dynlt1c* | dynein light chain Tctex-type 1C |
| 5.087358681 | 1.59584E-05 | 0.08971142 | *Eif4enif1* | eukaryotic translation initiation factor 4E nuclear import factor 1 |
| 2.267973449 | 3.78227E-12 | 1.27574E-07 | *9530068E07Rik* | RIKEN cDNA 9530068E07 gene |
| 1.89063498 | 8.09421E-06 | 0.054602732 | *Mylk* | myosin, light polypeptide kinase |
| 1.184307257 | 2.05084E-05 | 0.098819929 | *Sltm* | SAFB-like, transcription modulator |
| 1.169578801 | 7.58039E-06 | 0.054602732 | *Uba1* | ubiquitin-like modifier activating enzyme 1 |
| 1.125582966 | 4.30911E-06 | 0.036335998 | *Bahcc1* | BAH domain and coiled-coil containing 1 |
| -1.28013971 | 3.83611E-06 | 0.036335998 | *Cyld* | CYLD lysine 63 deubiquitinase |

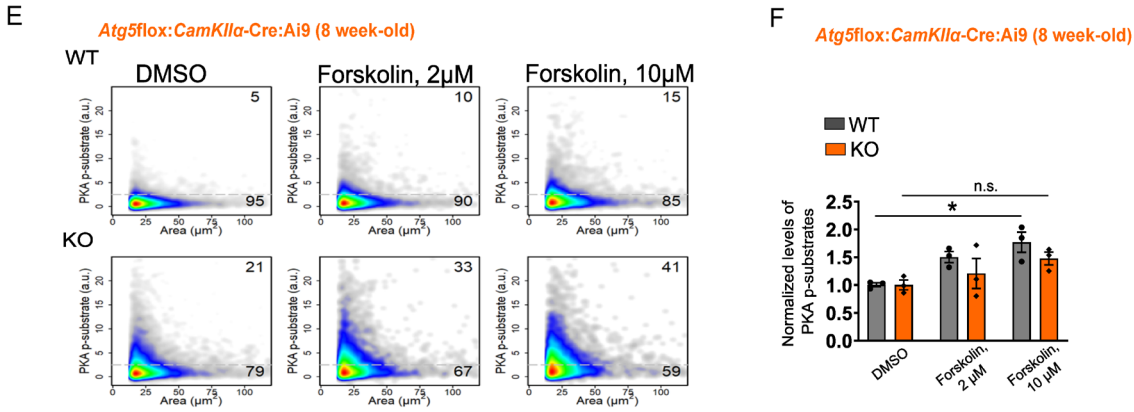


**Appendix Figure S7 | cAMP levels are unaltered in the cortex and hippocampus of *Atg5*flox:*CamKIIα*-Cre KO mice.** (**A**) Levels of cAMP are unaltered in the hippocampus of *Atg5*flox:*CamKIIα*-Cre KO mice compared to the WT (WT: 5.34±0.711, KO: 4.33±1.01). p=0.445, n=4. Performed two-tailed unpaired t-test. **(B, C)** High-content screening microscopy analysis detects no alterations in cAMP fluorescence intensity in cortical neurons isolated from 8-week-old *Atg5*flox:*Slc32a1*-Cre:*Ai9* WT and KO mice (WT: 1.30±0.305, KO: 0.784±0.172). p= 0.213, n=3. Performed two-tailed unpaired t-test. **(D)** Differentially expressed genes (FDR<1)

identified in mRNA sequencing analysis of 3-week- old *Atg5*flox:*CamKIIα*-Cre:*Ai9* FACS sorted WT and KO neurons (Sleuth-based analysis of Kalisto transcriptome output, see also Dataset EV3). **(E, F)** High-content screening microscopy analysis of cortical neurons isolated from 8-10-week-old *Atg5*flox:*CamKIIα*-Cre:*Ai9* mice and immunostained with RRXS/T motif antibody to visualize phosphorylated PKA substrates. Forskolin stimulation increased levels of RRXS/T motif-carrying proteins in WT, but not in KO neurons ($WT_{DMSO}$: 1.005±0.034, $KO_{DMSO}$: 1.004±0.086, $WT_{Forskolin\ 2\mu M}$: 1.502±0.098, $KO_{Forskolin\ 2\mu M}$: 1.209±0.269, $WT_{Forskolin\ 10\mu M}$: 1.770±0.182, $KO_{Forskolin\ 10\mu M}$: 1.476±0.116). $p_{WT\ DMSO/WT\ Forskolin\ 10\mu M}$= 0.034, n=3. Performed Two-Way ANOVA with Tukeys' multiple comparison test.

Data information: *P < 0.05; **P < 0.01; ***P < 0.001. All data represent mean ± SEM. All n represent biological replicates.

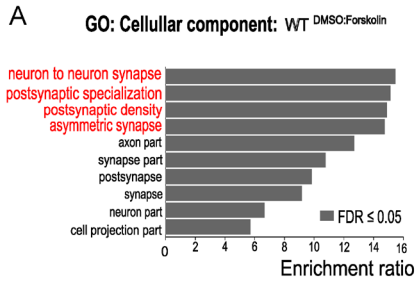


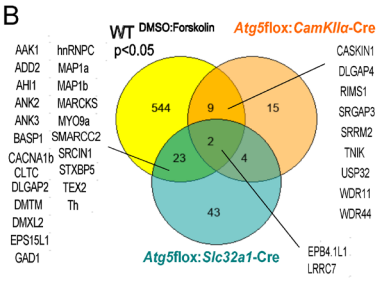


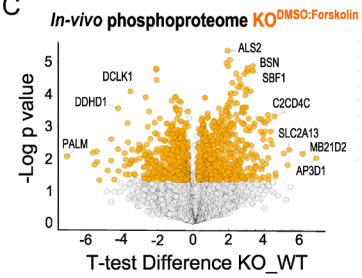


D

| Proteins | Putative PKA phosphorylaiton motif | Position within proteins | Amino acid | -Log Student's T-test p-value KO_For_KO_ DMSO | Student's T-test Difference KO_For_KO_ DMSO | -Log Student's T-test p-value WT_For_WT_ DMSO | Student's T-test Difference WT_For_WT_ DMSO |
|---|---|---|---|---|---|---|---|
| AAK1 | ASLNKSKSATTTPSGSPRTSQQNVSNASEGS | 595 | S | 0.879836 | 3.33887 | 1.79631 | 5.13112 |
| AHI1 | SETLYRDSPPKVKERSPPLTPKEKTKPEKPL | 974 | S | 0.690008 | 0.45567 | 1.98065 | 0.663725 |
| BASP1 | DKDKKAEGAGTEEEGTPKESEPQAAADATEV | 36 | T | 3.15587 | 0.454712 | 2.51292 | 0.796409 |
| BASP1 | ESEPQAAADATEVKESTEEKPKDAADGEAKA | 54 | S | 1.05553 | 0.184701 | 1.77585 | 0.642271 |
| CACNA1B | GGAIQTQESGIKESLSWGTQRTQDALYEARA | 1930 | S | 0.192919 | 0.0985151 | 1.49221 | 0.40685 |
| CASKIN1 | AEDGRLGVRAQRRRASDLAGSVDTGSAGSVK | 989 | S | 3.18353 | 1.56807 | 2.79075 | 2.04697 |
| DMTN | LQNGEGQRGRMDRGNSLPCVLEQKIYPYEML | 1048 | S | 0.258769 | -0.590454 | 3.23693 | 0.705419 |
| DLGAP2 | RAASFRQNSATERADSIEIYIPEAQTRL___ | 333 | S | 1.0426 | 0.441275 | 1.68103 | 0.500022 |
| HNTNPC | VEMKNEKSEEEQSSASVKKDETNVKMESEAG | 229 | S | 0.288494 | 0.176146 | 1.48393 | 0.450926 |
| LRRC7 | GPQPGRCLIQTKGQRSMDGYPEQFCVRIEKN | 1390 | S | 0.559194 | 0.372772 | 1.88971 | 0.620244 |
| MAP1B | PFEGKNGKQGFPDRESPVSDLTSTGLYQDKQ | 1438 | S | 0.831848 | 0.324025 | 1.69159 | 0.40914 |
| MAP1B | KEECPRPMSISPPDFSPKTAKSRTPVQDHRS | 1621 | S | 0.597307 | 0.169177 | 1.721 | 0.399388 |
| MYO9A | SKESPDKQQERGRRQSGTDLQEDVIVRQRPK | 1243 | S | 1.79526 | 2.20995 | 2.07795 | 2.80921 |
| RIMS1 | RMHARVSRARHERRHSDVALPHTEAAAAVSA | 413 | S | 0.884137 | 1.58015 | 3.88045 | 3.52221 |
| SRRM2 | RRGRSHSRSPATRGRSRSRTPARRGRSRSRT | 302 | S | 0.339255 | -1.01368 | 1.31222 | 3.93366 |
| SRRM2 | GRSHSRSPATRGRSRSRTPARRGRSRSRTPA | 58 | T | 1.56997 | 0.921431 | 1.68049 | 2.04425 |
| SRCIN1 | RFSNVGLVHTSERRHTVIAAQSLEALSGLQK | 474 | S | 0.359278 | -1.57167 | 1.52985 | 3.64302 |
| SMARCC2 | DRRDKKGGNYKKRKRSPSPSPTPEAKKKNAK | 476 | S | 0.465461 | -2.15655 | 1.39088 | 3.31237 |
| STXBP5 | SKMVANDLAKMSRKLSLPTDLKPDLDVKDNS | 760 | S | 2.06433 | 0.727748 | 1.60031 | 1.10867 |
| TH | QAEAVTSPRFIGRRQSLIEDARKEREAAAAA | 40 | S | 1.4279 | 1.42353 | 2.0676 | 1.98391 |

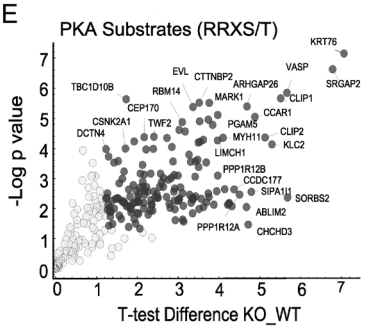


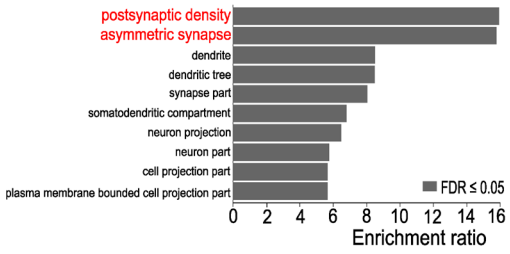


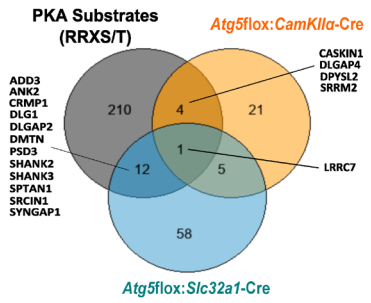


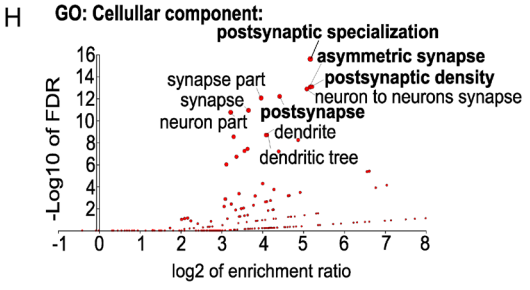


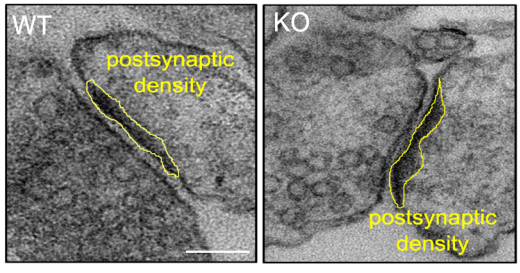


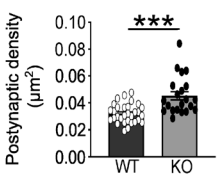


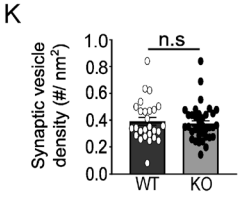

**Appendix Figure S8 | PKA targets are enriched at the PSD of excitatory synapses. (A)** WebGestalt-based GO analysis of "cellular component"-enriched terms in the phosphoproteome of Forskolin-treated WT brain slices (see Fig. 6E). **(B)** Venn diagram showing the number of phosphopeptides significantly downregulated in *Atg5*flox:*CamKIIα*-Cre and *Atg5*flox:*Slc32a1*-Cre KO brains (cut-off $p<0.05$, Fold change <-1.2) and significantly upregulated in WT brain slices upon Forskolin (50µM, 15 min treatment) (cut-off $p<0.05$, Fold change >1.2). **(C)** Volcano plot of differentially expressed phosphopeptides in acute *Atg5*flox:*CamKIIα*-Cre KO brain slices treated either with DMSO as control or 50µM Forskolin for 15 min. Highlighted are the proteins with $p<0.05$ and a 1.2/-1.2 minimal fold-change (log2FC ±0.58). n=5 each. **(D)** Numeric overview of putative PKA targets downregulated in ATG5 KO brains compared to WT, which are shown in Fig. 6F. **(E)** Volcano plot of co-immunoprecipitated PKA substrates in WT brain using the RRXS/T motif antibody. Highlighted are significant proteins ($p<0.05$) with a FC>1.2, n=4. See also Dataset EV4. **(F)** WebGestalt-based GO analysis of "cellular component"-enriched terms in all proteins highlighted in (E). **(G)** Venn diagram showing the number of putative PKA substrates detected using the co-immunoprecipitation analysis in (E) and phosphopeptides significantly downregulated in *Atg5*flox:*CamKIIα*-Cre KO and *Atg5*flox:*Slc32a1*-Cre KO brains (cut-off $p<0.05$, Fold change <-1.2). **(H)** WebGestalt- based GO analysis of "cellular component" enriched terms among common proteins identified (G). **(I)** Representative EM pictures showing a *Atg5*flox:*CAG*-$Cre^{Tmx}$ WT/ KO pre- and postsynapse. Scale bar: 120 nm. **(J)** EM analysis of the postsynaptic density thickness showed an increase in *Atg5*flox:*CAG*-$Cre^{Tmx}$ WT and KO cortico-hippocampal neurons (WT: 0.032± 0.001, KO: 0.045± 0.003; $p<0.0001$, two-tailed unpaired t-test). $n_{WT}=31$, $n_{KO}=21$ synapses from n=3 independent experiments. **(K)** No changes in the synaptic vesicle density (number of vesicles normalized to the area ($nm^2$)) were observed (WT: 0.392± 0.030, KO: 0.376± 0.021; $p=0.653$, two-tailed unpaired t-test). $n_{WT}=27$, $n_{KO}=36$ synapses from n=3 independent experiments. Data information: *P < 0.05; **P < 0.01; ***P < 0.001. All data represent mean ± SEM. All n represent biological replicates.

.

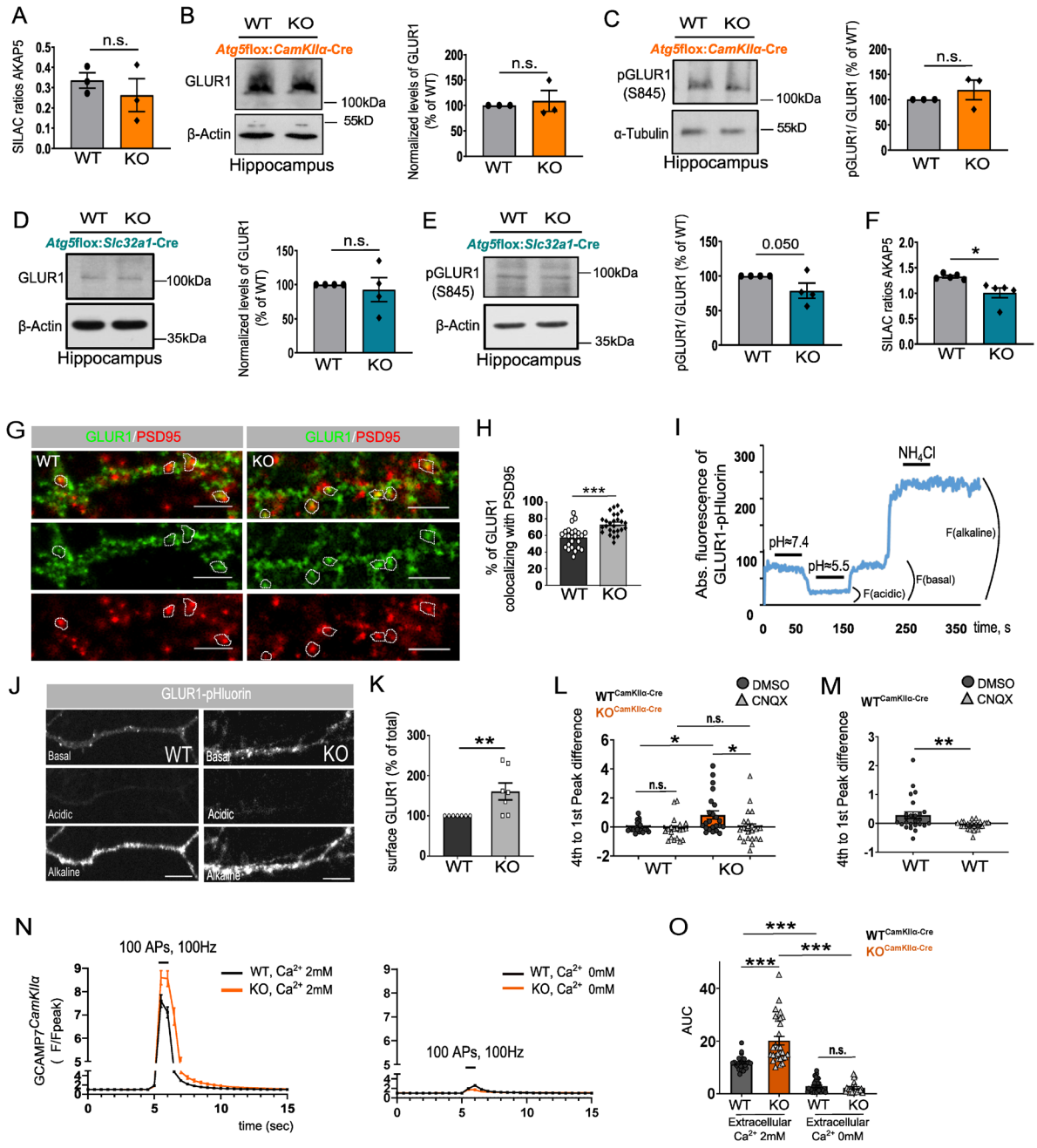


**Appendix Figure S9 | GLUR1 accumulates at the PSD95 of ATG5 KO neurons, whereas its total levels and/or phosphorylation state are not affected by autophagy deficiency.**

**(A)** SILAC-based proteome analysis does not reveal changes in AKAP5 (AKAP79) protein levels in *Atg5*flox:*CamKIIα*-Cre KO mice comparing to the WT (SILAC ratios, WT: 0.336±0.039, KO: 0.262±0.0805; p=0.458, two-tailed unpaired t-test). n=3 mice per genotype. **(B)** Total protein levels of GLUR1 are unaltered in *Atg5*flox:*CamKIIα*-Cre hippocampal lysates of KO mice (WT

set to 100%, KO: 108.9±20.47%; p=0.343, one-tailed unpaired t-test). n=3 mice per genotype. **(C)** Protein levels of phosphorylated GLUR1 (S845), normalized to total GLUR1 protein level, are unaltered in *Atg5*flox:*CamKIIα*-Cre hippocampal KO brain lysates compared to WT (WT set to 100%, KO: 119.1±19.31%; p=0.189, one-tailed unpaired t-test). n=3 mice per genotype. **(D)** Total protein levels of GLUR1 are unaltered in *Atg5*flox:*Slc32a1*-Cre hippocampal KO lysates compared to the WT (WT set to 100%, KO: 92.74±17.48; p=0.3462, one-tailed unpaired t-test). n=4 mice per genotype. **(E)** Protein levels of phosphorylated GLUR1 (S845), normalized to total GLUR1 protein level, are slightly reduced in hippocampal brain lysates of *Atg5*flox:*Slc32a1*-Cre KO mice compared to WT (WT set to 100%, KO: 78.86±10.88; p=0.050, one-tailed unpaired t-test). n=4 mice per genotype. **(F)** SILAC-based proteome analysis identifies alterations in AKAP5 (AKAP79) protein levels in *Atg5*flox:*Slc32a1*-Cre KO brain lysates compared to the (SILAC ratios, WT: 1.325±0.023, KO: 1.008±0.096; p=0.013, two-tailed unpaired t-test). n=5 mice per genotype. **(G)** Representative images of GLUR1 and PSD95 immunostaining in *Atg5*flox:*CAG*-$Cre^{Tmx}$ cortico-hippocampal neurons. White circles indicate PSD95 and GLUR1 colocalization in WT/ KO. Scale bar: 5µm. **(H)** Analysis of GLUR1 and PSD95 colocalization (% of GLUR1 puncta colocalizing with PSD95) in cultured *Atg5*flox:*CAG*-$Cre^{Tmx}$ WT and KO neurons at DIV14 (WT: 57.46±2.77%, KO: 73.62±2.27%; p<0.0001, unpaired two-tailed t-test) $n_{WT}$=23, $n_{KO}$=26 images from n=3 independent experiments. Analysis was performed using a custom-written Plugin for ImageJ (Data S2). **(I)** An example trace of GLUR1 pHluorin fluorescence upon exposure to buffer containing 25 mM MES at pH 5.5 and 50 mM $NH_4Cl$ at pH 7.4. Exposure to pH 5.5 quenches GLUR1 pHluorin fluorescence on the dendrite surface (plasma membrane), and application of $NH_4Cl$ raises the intravesicular pH to 7.4, thereby dequenching vesicular GLUR1 pHluorin fluorescence (total GLUR1 pHluorin). **(J)** Representative images of GLUR1 pHluorin fluorescence at the dendrite upon different buffer conditions in *Atg5*flox:*CAG*-$Cre^{Tmx}$ WT/KO cultured neurons. Scale bar: 5 µm. **(K)** Analysis of GLUR1 surface fraction in *Atg5*flox:*CAG*-$Cre^{Tmx}$ WT/KO transfected with GLUR1-pHlourin. The surface levels of GLUR1-pHlourin normalized to GLUR1-pHluorin total levels determined from the difference in fluorescence intensity between acidic and alkaline buffer conditions (WT set to 100 %, KO: 160.8±21.08%, p=0.0069, unpaired one-tailed t-test). $n_{WT}$=35, $n_{KO}$=30 neurons from n=7 independent experiments. **(L)** GCAMP7f responses to tetanic stimulation (four tetani, 100 APs at 100Hz, 3s interval) in *Atg5*wt:wt/*Ai9*+*CamKII*α-Cre (WT) and *Atg5*flox:flox/*Ai9*+*CamKII*α-Cre (KO)

dendrites from cortical-hippocampal neurons expressing m*CamKII*α-jGCaMP7f and treated either with DMSO or 10 μM CNQX for 5 min. ATG5-deficient dendrites show significantly increased facilitation of GCAMP7f signal to electrical stimulation (ΔF/Fpeak1) compared to WT, a phenotype which was blocked by the application of CNQX ($WT_{DMSO}$: -0.027± 0.075, $WT_{CNQX}$: -0.125±0.172, $KO_{DMSO}$: 0.824± 0.280, $KO_{CNQX}$: -0.0288± 0.240, $p_{WT\ DMSO/KO\ DMSO}$=0.0239, $p_{KO\ DMSO/KO\ CNQX}$=0.0235, two-way ANOVA with Tukey's multiple comparisons test, $n_{WT\ DMSO}$= 22, $n_{WT\ CNQX}$= 20, $n_{KO\ DMSO}$= 23, $n_{KO\ CNQX}$= 22 neurons from n=4 independent experiments. **(M)** Analysis of 4$^{th}$ to 1$^{st}$ peak difference of WT cells expressing GCAMP7$^{CamKII\alpha}$ treated with DMSO or CNQX show a decreased calcium response to electrical field stimulation (WT: 0.282± 0.117, KO: -0.070± 0.027; p=0.004, two-tailed unpaired t-test). $n_{WT}$=25, $n_{WT\ CNQX}$=27 neurons from n=3 independent experiments. **(N)** GCAMP7f responses to single pulse stimulation (100 APs at 100Hz) in *CamKII*α-Cre-transduced primary cortico-hippocampal *Atg5*wt:wt/*Ai9* (WT) and *Atg5*flox:flox/*Ai9* (KO) neurons expressing m*CamKII*α-jGCaMP7f in imaging buffer supplemented either with 2mM or 0mM extracellular $Ca^{2+}$. **(O)** Quantification of the area under the curve (AUC) of the GCAMP7f responses in electrically stimulated (100 action potentials at 100Hz) *Atg5*wt:wt/*Ai9*+*CamKII*α-Cre (WT) and *Atg5*flox:flox/*Ai9*+*CamKII*α-Cre (KO) dendrites in either 2mM or 0mM external $Ca^{2+}$ ($WT_{2mM}$: 11.72± 0.468, $WT_{0mM}$: 2.854±0.399, $KO_{2mM}$: 20.18± 1.640, $KO_{0mM}$: 2.219± 0.439; $p_{WT\ 2mM/WT\ 0mM}$<0.0001, $p_{WT\ 2mM/KO\ 2mM}$<0.0001, $p_{KO\ 2mM/KO\ 0mM}$<0.0001, $p_{WT\ 0mM/KO\ 0mM}$=0.726, two-way ANOVA with Tukey's multiple comparisons test). $n_{WT\ 2mM}$= 27, $n_{WT\ 0mM}$= 34, $n_{KO\ 2mM}$= 29, $n_{KO\ 0mM}$= 23 neurons from n=2 independent experiments. Data information: *P < 0.05; **P < 0.01; ***P < 0.001. All data represent mean ± SEM. All n represent biological replicates.

**Appendix Table S1: Primers used for genotyping of genetically modified mice used in the current study.**

| Gene | Sequence (5'- 3') |
|---|---|
| ***Atg5*** | |
| *Atg5* forward 1 | GAA TAT GAA GCC ACA CCC CTG AAA TG |
| *Atg5* forward 2 | ACA ACG TCG AGC ACG CTG GCG AAG G |
| *Atg5* reverse | GTA CTG CAT AAT GGT TTA ACT CTT GC |
| ***Atg16L1*** | |
| *Atg16L1_1* | CAG AAT AAT TTC CGG CAG AGA CCG G |
| *Atg16L1_2* | AGC CAA AGA AGG AAG GTA AGC AAC GAA |
| ***Cre*** | |
| *Cre_1* | GAA CCT GAT GGA CAT GTT CAG G |
| *Cre_2* | AGT GCG TTC GAA CGC TAG AGC CTG T |
| *Cre_3* | TTA CGT CCA TCG TGG ACA |
| *Cre_4* | TGG GCT GGG TGT TAG CC |
| ***tdTomato*** | |
| *tdTomato_1* | AAG GGA GCT GCA GTG GAG TA |
| *tdTomato_2* | CCG AAA ATC TGT GGG AAG TC |
| *tdTomato_3* | GGC ATT AAA GCA GCG TAT CC |
| *tdTomato_4* | CTG TTC CTG TAC GGC ATG G |

**Appendix Table S2:** Plasmid DNA used for transfection of cells *in-vitro* in the current study.

| Plasmid (source gene) | Manufacturer | Identifier |
|---|---|---|
| GFP | Clontech | pT3027.5 |
| pEGFP-C1-hAPG5 (ATG5-GFP) | addgene | #22952 |
| pcDNA3-mouse PKA-RIalpha-mEGFP | addgene | #45525 |
| pcDNA3-mouse PKA-RIbeta-mEGFP | addgene | #45526 |
| pCMV-SEP-GluA1 | addgene | #64942 |
| AKARet-PSD95 | addgene | #114732 |

**Appendix Table S3:** AAVs used for transfection of primary neurons in the current study.

| Name | Full description | Manufacturer | Identifier |
|---|---|---|---|
| eGFP $^{CamKII\alpha}$ | AAV9.CamKIIα0.4.eGFP.WPRE.rBG | Penn Vector Core | 105541 |
| eGFP-Cre $^{CamKII\alpha}$ | AAV9.CamKIIα.HI.eGFP-Cre.WPRESV40 | Penn Vector Core | 105551 |
| Cre $^{GAD67}$ | ssAAV-5/2-hGAD67-chl-iCre-SV40p(A) | Viral Vector Facility VVF | V197-5 |
| Cre $^{CamKII\alpha}$ | ssAAV-9/2-mCaMKIIα-iCre-WPRE-hGHp(A) | Viral Vector Facility VVF | V206-9 |
| GCAMP7f $^{CamKII\alpha}$ | ssAVV-9/2-mCaMKIIα-jGCaMP7f-WPREbGHp(A) | Viral Vector Facility VVF | V493-9 |

**Appendix Table S4:** Antibodies & DNA labelling dyes and their used concentration in Immunoblotting (WB), Immunocytochemistry (ICC), Immunohistochemistry (IHC) and Immunoprecipitation (IP) analysis.

| **Antibodies** | **Used concentration** | | | | **Manufacturer** | **Catalog number** |
|---|---|---|---|---|---|---|
| **Target protein** | WB | ICC | IHC | IP | | |
| ATG5 | 1:1000 | - | - | - | Abcam | ab108327 |
| β-Actin | 1:1000 | - | - | - | Sigma | A-5441 |
| Bassoon | - | - | 1:500 | - | Synaptic Systems | 141002 & 141004 |
| CREB | 1:1000 | - | - | - | Cell Signaling | 9197 |
| cAMP | - | 1:500 | - | - | Abcam | ab24856 |
| CASKIN1 | - | 1:300 | - | - | Synaptic Systems | 185 002 |
| GAPDH | 1:1000 | - | - | - | Sigma-Aldrich | G8795 |
| GFP | - | 1:2000 | 1:1000 | - | Abcam | ab13970 |
| GLUA1 | 1:1000 | 1:500 | 1:500 | - | Synaptic Systems | 182011 |

| | | | | | | |
|---|---|---|---|---|---|---|
| Glutamate receptor 1 (AMPA subtype) phospho S845 | 1:1000 | - | - | - | Abcam | ab76321 |
| LC3B | 1:2000 | - | - | - | Novus Biologicals | NB600-1384SS |
| MAP2 | - | 1:500 | - | - | Sigma-Aldrich | M9942 |
| mCherry | - | - | 1:2000 | - | Abcam | ab167453 |
| NBR1 | - | - | 1:300 | - | Santa Cruz Biotechnology | sc-130380 |
| Normal Rabbit IgG | - | - | - | 2 µg | Cell Signaling | 2729 |
| Normal Mouse IgG | - | - | - | 2 µg | Millipore | 12-371 |
| Normal Sheep IgG | - | - | - | 2 µg | Jackson Immuno Research | 713-005-147 |
| p62 | 1:1000 | 1:1000 | 1:1000 | - | Progen | GP62-C |
| pCREB (Ser133) | 1:1000 | 1:500 | - | - | Cell Signaling | 9198 |
| pCREB (S133) | - | 1:500 | - | - | Thermo Fisher (Pierce) | MA5-11192 |
| pGluR1 (S845) | 1:1000 | - | - | - | Abcam | ab76321 |
| pPKA R2α | - | 1:500 | - | - | Abcam | ab32390 |
| pPKA-Substrate | 1:1000 | - | - | 2 µg | Cell Signaling | 9624 |
| PKA Cα | 1:1000 | - | - | - | Cell Signaling | 5842 |
| PKA R1α | 1:1000 | 1:300 | 1:300 | 2 µg | Cell Signaling | 5675 |
| PKA R1α/β | 1:1000 | - | - | - | Cell Signaling | 3927 |
| PKA R1β | 1:1000 | 1:300 | 1:300 | 2 µg | R&D Systems | AF4177 |
| PKA R2α | 1:1000 | - | - | - | BD Transduction Laboratories | 612242 |
| PKA R2β | 1:1000 | - | - | - | Abcam | Ab32390 |
| PSD95 | - | 1:300 | 1:300 | - | Synaptic Systems | 124 008 |

| | | | | | | |
|---|---|---|---|---|---|---|
| S6 Ribosomal Protein (phosho Ser235/236) | 1:1000 | - | - | - | Cell Signaling | 2211 |
| SHANK3 | - | 1:300 | - | - | Cell Signaling | 64555 |
| α-Tubulin | 1:1000 | - | - | - | Synaptic Systems | 302 211 |
| Vinculin [EPR8185] | 1:1000 | - | - | - | Abcam | ab129002 |
| **DNA labelling dyes** | | | | | | |
| DAPI | - | 1:10000 | - | - | Roth | 6335.1 |
| DRAQ5 | - | 1:1000 | - | - | Thermo Scientific | 62254 |

**Appendix Table S5: Secondary antibodies with HRP (WB) or fluorescence (ICC / IHC) tag and their used concentration.**

| **Antibody target** | **Used concentration** | | | **Manufacturer** | **Catalog number** |
|---|---|---|---|---|---|
| | WB | ICC | IHC | | |
| Goat anti-Mouse IgG (H+L) peroxidase-conjugated | 1:5000 | - | - | Jackson Immuno Research | 115-035-003 |
| Goat anti-Rabbit IgG (H+L) peroxidase-conjugated | 1:5000 | - | - | Jackson Immuno Research | 111-035-003 |
| Goat anti-Guinea Pig IgG (H+L) peroxidase-conjugated | 1:5000 | - | - | Jackson Immuno Research | 106-035-003 |
| Goat anti-Sheep IgG (H+L) peroxidase-conjugated | 1:5000 | - | - | Invitrogen | A16041 |
| Alexa Fluor 488 Goat anti-Mouse IgG | - | 1:500 | - | Life Technologies GmbH | A11029 |
| Alexa Fluor 488 Goat anti-Rabbit IgG | - | 1:500 | 1:500 | Life Technologies GmbH | A11034 |
| Alexa Fluor 488 Goat anti-Chicken IgG | - | 1:500 | 1:500 | Life Technologies GmbH | A11039 |

| | | | | | |
|---|---|---|---|---|---|
| Alexa Fluor 488 Goat anti-Guinea Pig IgG | - | 1:500 | 1:500 | Life Technologies GmbH | A11073 |
| Alexa Fluor 488 Donkey anti-Sheep IgG | | 1:500 | 1:500 | Life Technologies GmbH | A11015 |
| Alexa Fluor 568 Goat anti-Mouse IgG | - | 1:500 | 1:500 | Life Technologies GmbH | A-11031 |
| Alexa Fluor 568 Goat anti-Rabbit IgG | - | 1:500 | 1:500 | Life Technologies GmbH | A11036 |
| Alexa Fluor 568 Goat anti-Guinea Pig IgG | - | 1:500 | 1:500 | Life Technologies GmbH | A11075 |
| Alexa Fluor 568 donkey anti-mouse IgG | - | 1:500 | 1:500 | Life Technologies GmbH | A10037 |
| Alexa Fluor 555 Donkey anti-Sheep IgG | - | 1:500 | 1:500 | Life Technologies GmbH | A21436 |
| Alexa Fluor 647 Goat anti-Mouse IgG | - | 1:500 | 1:500 | Life Technologies GmbH | A21236 |
| Alexa Fluor 647 Goat anti-Mouse IgG | - | 1:500 | - | Life Technologies GmbH | A327728 |
| Alexa Fluor 647 Goat anti-Rabbit IgG | - | 1:500 | 1:500 | Life Technologies GmbH | A21245 |
| Alexa Fluor 647 Goat anti-Guinea Pig IgG | - | 1:500 | 1:500 | Life Technologies GmbH | A21450 |
| Alexa Fluor 647 Donkey anti-Rabbit IgG | - | 1:500 | 1:500 | Life Technologies GmbH | A31573 |
| Alexa Fluor 488 F(ab')2 Fragment goat anti-mouse | - | 1:500 | - | Life Technologies GmbH | A11017 |

| | | | | | |
|---|---|---|---|---|---|
| ATTO647N goat anti-rabbit | - | 1:500 | - | Sigma Aldrich | 40839-1ML-F |